

Penetrability in model colloid–polymer mixtures

Matthias Schmidt

Institut für Theoretische Physik, Heinrich-Heine Universität Düsseldorf, Universitätsstraße 1, D-40225 Düsseldorf, Germany

Matthias Fuchs^{a)}

Institut Charles Sadron, 6, rue Boussingault, 67083 Strasbourg Cedex, France

(Received 3 May 2002; accepted 5 July 2002)

In order to study the effects of penetrability in mixtures of dissimilar particles we consider hard (colloidal) spheres and penetrable spheres. The latter may be taken to represent ideal, noninteracting polymer coils. Polymers and colloids interact by means of a repulsive step-function pair potential, which allows for insertion of colloids into the polymer coil. The potential strength is obtained from scaling arguments for the cross virial coefficient of true colloid–polymer systems. For this model we construct a geometry-based density functional and apply it to bulk fluid demixing. We find that taking into account penetrability leads to a significant stabilization of the mixed phase for large polymer-to-colloid size ratio. © 2002 American Institute of Physics. [DOI: 10.1063/1.1503303]

I. INTRODUCTION

Different levels of description have been used to study the emergence of structure and phase behavior in colloid–polymer mixtures. Such systems are experimentally well characterized and the phase behavior typically displays (colloid) gas, liquid and crystalline phases. A coarse-grained level of description relies on effective spheres to model globular nonadsorbing polymers and goes back to Asakura and Oosawa (AO) (Ref. 1) and Vrij.² Perturbation theory,³ free volume theory,^{4,5} and simulations^{5,6} have been successfully employed to study the bulk properties of this model.

A deeper, more microscopic level of description is the basis for theories that operate on the blob⁷ or segment^{8–11} level of the polymers. It has also been the basis for computer simulations of colloidal spheres and lattice polymers.^{12–14} While these approaches consider translational *and* conformational (internal) contributions to the entropy, a reduction of the degrees of freedom to the center-of-mass translations of both species would among other advantages for example greatly speed up computer simulations of these complex mixtures. This aim has recently been pursued using soft sphere approaches to polymers^{15,16} and also motivates our study.

Density functional theory (DFT) (Ref. 17) is more powerful than the above bulk theories, as it is capable of dealing with *inhomogeneous* situations. In the context of effective sphere models previous hard sphere theories^{18,19} could be extended to a range of models, including the AO model without^{20,21} and with polymer–polymer interactions.²² Interesting inhomogeneous situations are realized in interfaces between demixed fluid states and near walls, where wetting and layering phenomena were found.²³

In this work we use effective polymer spheres and do one step towards a more realistic description by allowing

colloids to penetrate the polymer spheres. On the segment level (disregarded within our model), this leads to a restriction of allowed polymer configurations, hence a free energy penalty emerges. We calculate its strength from the cross virial coefficient and use this as an input for the effective sphere model, by setting the free energy penalty equal to an *internal* energy contribution to the Hamiltonian, both for a theta solvent and for a good solvent. As an approximation, we disregard polymer–polymer interactions, as would be justified for dilute polymers and at the theta temperature. We derive a DFT for the model and apply it to bulk fluid demixing. For small polymer-to-colloid size ratios the demixing binodal approaches the free volume result for impenetrable polymer.⁴ In the opposite regime of large polymer-to-colloid size ratios, our theory predicts a significant stabilization of the mixed fluid phase, the effect being stronger in the case of a good solvent.

We specify the model of hard colloids and penetrable polymer in Sec. II, and develop the theory in Sec. III. Bulk fluid–fluid demixing is calculated in Sec. IV and we finish with concluding remarks in Sec. V.

II. THE MODEL

We consider a mixture of colloidal particles (species *C*) and effective polymer spheres (species *P*) interacting by means of pair potentials $V_{ij}(r)$, where $i, j = C, P$, see Fig. 1 for a sketch of the model. The interactions between particles of the same species are

$$V_{CC}(r) = \begin{cases} \infty & \text{if } r < 2R_C \\ 0 & \text{else,} \end{cases} \quad (1)$$

$$V_{PP}(r) = 0. \quad (2)$$

The interaction between colloids and polymers is

$$V_{CP}(r) = \begin{cases} \epsilon_{CP} & \text{if } r < R_C + R_P \\ 0 & \text{else.} \end{cases} \quad (3)$$

^{a)}Permanent address: Physik Department, Technische Universität München, D-85747 Garching, Germany.

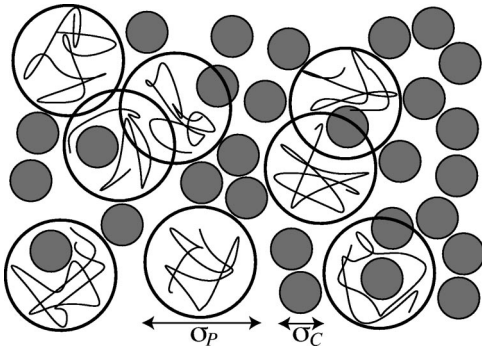


FIG. 1. Sketch of the model with hard colloidal spheres of diameter $\sigma_C = 2R_C$ and effective polymer spheres with diameter $\sigma_P = 2R_P$. Penetration of colloids into polymers is accompanied by an energy cost ϵ_{CP} .

In essence, this is the AO model where the the colloid–polymer interaction is assumed to be penetrable rather than hard. Hence we refer to this model as the penetrable Asakura–Oosawa (PAO) model. The PAO model reduces in the limit $\beta\epsilon_{CP} \rightarrow \infty$ to the classic AO model,^{1,2} where $\beta = 1/k_B T$, k_B is the Boltzmann constant, and T is absolute temperature. Another (albeit trivial) limit is obtained for $\beta\epsilon_{CP} \rightarrow 0$ (and finite radii R_P, R_C), where the mixture decouples into a hard sphere colloid fluid and an ideal gas of polymers; these subsystems do not interact with each other.

As bulk thermodynamic parameters we use the packing fractions $\eta_C = 4\pi R_C^3 \rho_C / 3$, $\eta_P = 4\pi R_P^3 \rho_P / 3$, where ρ_C, ρ_P are the number densities of colloids and polymers, respectively. The system volume is denoted by V . The size ratio $q = R_P / R_C$ and the (reduced) strength $\beta\epsilon_{CP}$ act as control parameters.

III. THEORY

A. Zero-dimensional limit

In order to work out a density functional theory for the PAO model we follow the lines suggested in Refs. 18 and 19 for hard spheres and in Refs. 20–22, 24, and 25 for a broader class of models and determine the excess Helmholtz free energy from dimensional crossover starting with the zero-dimensional (0D) limit. The 0D limit corresponds to the problem of packing particles into cavities such that all particles overlap. This is an idealized situation and allows for an exact solution of the many-body problem. To obtain the 0D grand partition sum, Ξ , we count the possible states characterized by the particle numbers of colloids and polymers (which can be regarded as occupancy numbers of the 0D cavity). As we deal with a thermal system, where $\beta\epsilon_{CP}$ is a control parameter, we need to consider the appropriate statistical weight, given by the Boltzmann factor, in the grand ensemble. Summing-up the possible states, we have (i) all states with an arbitrary number of polymers but without colloids. This includes the empty state with vanishing particle numbers, and essentially constitutes the partition sum of an ideal gas of polymers. Furthermore, we need to consider (ii) a single colloidal particle and an arbitrary number of polymers. All remaining states are characterized by at least two colloidal particles. Due to the hard core potential between

colloids, these states carry vanishing statistical weight. Hence we obtain the 0D grand partition sum,

$$\Xi = \exp(z_P) + z_C \exp(z_P \exp(-\beta\epsilon_{CP})), \quad (4)$$

where the first (second) term corresponds to case i (ii) above, and z_i is the fugacity of species $i = C, P$. From the grand partition sum Ξ , Eq. (4), the (canonical) Helmholtz free energy can be obtained by a (double) Legendre transform from the fugacities z_i to the mean numbers of particles $\bar{\eta}_i = z_i \partial \ln \Xi / \partial z_i$. Hence the excess (over ideal gas) free energy F_{0D} is obtained from $\beta F_{0D} + \bar{\eta}_P [\ln(\bar{\eta}_P) - 1] + \bar{\eta}_C [\ln(\bar{\eta}_C) - 1] = -\Xi + \bar{\eta}_P \ln(z_P) + \bar{\eta}_C \ln(z_C)$. The straightforward calculation gives

$$\beta F_{0D} = (1 - \bar{\eta}_C) \ln(1 - \bar{\eta}_C) + \bar{\eta}_C - \bar{\eta}_P \ln(1 - \bar{\eta}_C [1 - \exp(-\beta\epsilon_{CP})]). \quad (5)$$

It is instructive to consider the limit of weak colloid–polymer interactions, $\beta\epsilon_{CP} \rightarrow 0$. By Taylor expanding Eq. (5) one obtains

$$\beta F_{0D} = (1 - \bar{\eta}_C) \ln(1 - \bar{\eta}_C) + \bar{\eta}_C - \beta\epsilon_{CP} \bar{\eta}_P \bar{\eta}_C + O(\beta^2 \epsilon_{CP}^2). \quad (6)$$

The sum of the first two terms in Eq. (6) equals the 0D free energy of hard spheres.^{26,27} The next term is bilinear in the densities involved—a typical mean-field contribution. This might be expected on physical grounds. We stress, however, that Eq. (6) is an *exact* expansion. We further note that in the limit of hard colloid–polymer interaction, $\beta\epsilon_{CP} \rightarrow \infty$, the 0D free energy is $\beta F_{0D} = (1 - \bar{\eta}_C - \bar{\eta}_P) \ln(1 - \bar{\eta}_C) + \bar{\eta}_C$, equal to the result for the AO model.^{20,21}

B. Density functional theory

The total Helmholtz free energy of an inhomogeneous system may be written as $F = F_{id} + F_{exc}$, where $F_{id} = \sum_{i=C,P} \int d\mathbf{r} \rho_i(\mathbf{r}) [\ln(\rho_i(\mathbf{r}) \Lambda_i^3) - 1]$ is the ideal-gas free energy functional (for two species), with Λ_i being the (irrelevant) thermal wavelength of species i , and F_{exc} is the excess contribution arising from interactions between particles. Following previous work on mixtures,^{18,20,21,26,27} we express the Helmholtz excess free energy as a functional of colloid and polymer density fields as a spatial integral

$$F_{exc}[\rho_C(\mathbf{r}), \rho_P(\mathbf{r})] = k_B T \int d^3x \Phi(\{n_\nu^C(\mathbf{x})\}, \{n_\nu^P(\mathbf{x})\}), \quad (7)$$

where the weighted densities

$$n_\nu^i(\mathbf{x}) = \int d^3r \rho_i(\mathbf{r}) w_\nu^i(\mathbf{x} - \mathbf{r}), \quad i = C, P \quad (8)$$

are defined as convolutions of weight functions, w_ν^i , with the actual density profiles, and $\nu = 0, 1, 2, 3, v1, v2, m2$ denotes the type of weight function.

The weight functions w_ν^i are independent of the density profiles and are given by

$$w_3^i(\mathbf{r}) = \Theta(R_i - r), \quad w_2^i(\mathbf{r}) = \delta(R_i - r), \quad (9)$$

$$w_{v2}^i(\mathbf{r}) = w_2^i(\mathbf{r}) \mathbf{r} / r, \quad w_{m2}^i(\mathbf{r}) = w_2^i(\mathbf{r}) [\mathbf{r} \mathbf{r} / r^2 - \hat{\mathbf{1}} / 3], \quad (10)$$

where $r=|\mathbf{r}|$, $\Theta(r)$ is the step function, $\delta(r)$ is the Dirac distribution, and $\hat{\mathbf{1}}$ is the 3×3 identity matrix, and matrices are denoted by a hat. Further, linearly dependent, weights are $w_1^i(\mathbf{r})=w_2^i(\mathbf{r})/(4\pi R_i)$, $\mathbf{w}_{v1}^i(\mathbf{r})=\mathbf{w}_{v2}^i(\mathbf{r})/(4\pi R_i)$, $w_0^i(\mathbf{r})=w_1^i(\mathbf{r})/R_i$. The weight functions are quantities with dimension (length) $^{3-\nu}$. They differ in their tensorial rank: w_0^i , w_1^i , w_2^i , w_3^i are scalars; \mathbf{w}_{v1}^i , \mathbf{w}_{v2}^i are vectors; $\hat{\mathbf{w}}_{m2}^i$ is a (traceless) matrix.

The free energy density Φ is composed of three parts^{18,19} that arise from consideration of one, two and three cavities,²⁸

$$\Phi = \Phi_1 + \Phi_2 + \Phi_3. \quad (11)$$

They are defined as

$$\Phi_1 = \sum_{i=C,P} n_0^i \varphi_i(n_3^C, n_3^P), \quad (12)$$

$$\Phi_2 = \sum_{i,j=C,P} (n_1^i n_2^j - \mathbf{n}_{v1}^i \cdot \mathbf{n}_{v2}^j) \varphi_{ij}(n_3^C, n_3^P), \quad (13)$$

$$\begin{aligned} \Phi_3 = & \frac{1}{8\pi} \sum_{i,j,k=C,P} \left(\frac{1}{3} n_2^i n_2^j n_2^k - n_2^i \mathbf{n}_{v2}^j \cdot \mathbf{n}_{v2}^k \right. \\ & \left. + \frac{3}{2} [\mathbf{n}_{v2}^i \hat{\mathbf{n}}_{m2}^j \mathbf{n}_{v2}^k - \text{tr}(\hat{\mathbf{n}}_{m2}^i \hat{\mathbf{n}}_{m2}^j \hat{\mathbf{n}}_{m2}^k)] \right) \varphi_{ijk}(n_3^C, n_3^P), \end{aligned} \quad (14)$$

where tr denotes the trace, and m th order derivatives of the OD excess free energy [Eq. (5)] are

$$\varphi_{i\dots k}(\bar{\eta}_C, \bar{\eta}_P) \equiv \frac{\partial^m}{\partial \bar{\eta}_i \dots \partial \bar{\eta}_k} F_{\text{OD}}(\bar{\eta}_C, \bar{\eta}_P). \quad (15)$$

This completes the prescription for the functional.

C. Penetrable colloid–polymer interactions

The theory we have presented so far is applicable to arbitrary (constant) colloid–polymer interaction strength ϵ_{CP} and polymer-to-colloid size ratios q . As our aim is a study of the effects of particle–coil penetration in real colloid–polymer mixtures, we seek to find a relation between ϵ_{CP} and q to match our effective sphere system with the behavior of true polymers. In the following this is carried out for the case of low density of polymer and a single sphere, where we consider the excess chemical potential or insertion free energy. In lowest order, it is determined by the cross virial coefficient between colloid and polymer. We consider two cases, namely a theta solvent and a poor solvent, in order to also learn about the effect of excluded volume swelling of the coil structure. The excess insertion free energies for adding $V\rho_C$ independent spheres to a dilute solution of polymers, or to a solution of noninteracting polymers at arbitrary density, are known from field-theoretic considerations and satisfy scaling limits for large q ,^{29,30}

$$\begin{aligned} & \beta \delta F_{\text{exc}}/(V\rho_C) \\ & \rightarrow \begin{cases} 4\pi\rho_P R_P^3/q & \text{for } \nu = \frac{1}{2} \text{ (theta solvent)} \\ 18.461\rho_P R_P^3 q^{1/\nu-d} & \text{for } \nu = 0.588 \text{ (good solvent),} \end{cases} \end{aligned} \quad (16)$$

where $d=3$ is the space dimension. Particle insertion into

the polymer coil is manifest in the decrease of $\beta \delta F_{\text{exc}}$ for large q where the open polymer structure becomes important. Using the potential given in Eq. (3), the virial expansion is in the limit of small interactions $\beta \epsilon_{CP}$ given by $\beta \delta F_{\text{exc}}/(V\rho_C) \rightarrow \frac{4}{3}\pi R_P^3 \rho_P \beta \epsilon_{CP}$. Requiring this to agree with Eq. (16) in the limit of large polymers, we find for the theta solvent,

$$\beta \epsilon_{CP}(q) = \frac{3}{q}, \quad (17)$$

and in a good solvent

$$\beta \epsilon_{CP}(q) = \frac{4.40724}{q^{3-1/\nu}} = \frac{4.40724}{q^{1.29932}}, \quad (18)$$

where $\nu=0.588$.

There is a crossover between both functional forms for $\epsilon_{CP}(q)$. For smaller (larger) values than $q=3.615$, the interaction strength ϵ_{CP} is weaker in the case of a theta (good) solvent.

IV. RESULTS

A. Thermodynamics

To obtain the thermodynamics of homogeneous fluid states, we apply the density functional described in Sec. III B to constant density fields, $\rho_C(\mathbf{r})=\text{const}$, $\rho_P(\mathbf{r})=\text{const}$. In this case the scalar weighted densities n_ν^i , $\nu=3,2,1,0$ become proportional to the bulk densities, $n_\nu^i = \xi_\nu^i \rho_i$, where the proportionality constants ξ_ν^i are so-called fundamental measures obtained as $\xi_\nu^i = \int d^3r w_\nu^i(\mathbf{r})$ [see Eq. (8)]. Explicitly the fundamental measures are given as $\xi_3^i = 4\pi R_i^3/3$, $\xi_2^i = 4\pi R_i^2$, $\xi_1^i = R_i$, $\xi_0^i = 1$, corresponding to the volume, surface, integral mean curvature, and Euler characteristic of the spheres of species i . The vectorial and tensorial weighted densities, \mathbf{n}_{v2}^i , \mathbf{n}_{v1}^i , $\hat{\mathbf{n}}_{m2}^i$ vanish for constant density fields, due to the symmetry of the corresponding weight functions [Eq. (10)]. Inserting the obtained expressions for the n_ν^i into Eqs. (12)–(14), and carrying out the derivatives in Eq. (15) yields the excess free energy density Φ [Eq. (11)]. As Φ is also constant in space, the integration in Eq. (7) becomes trivial, and the bulk excess Helmholtz free energy density is obtained as

$$\beta F_{\text{exc}}/V = \beta \phi_{\text{HS}}(\rho_C) - \rho_P \ln \alpha_{\text{PAO}}(\rho_C), \quad (19)$$

where $\phi_{\text{HS}}(\rho_C)$ is the excess free energy per unit volume of pure HS in the scaled-particle (and Percus–Yevick compressibility) approximation, given as

$$\beta \phi_{\text{HS}}(\rho_C) = \frac{3\eta_C[3\eta_C(2-\eta_C) - 2(1-\eta_C)^2 \ln(1-\eta_C)]}{8\pi R_C^3(1-\eta_C)^2}, \quad (20)$$

and

$$\alpha_{\text{PAO}}(\rho_C) = (1-\eta'_C) \exp(-A\gamma - B\gamma^2 - C\gamma^3), \quad (21)$$

where $\gamma = \eta'_C/(1-\eta'_C)$, $\eta'_C = [1 - \exp(-\beta \epsilon_{CP})]\eta_C$, and the coefficients depend only on the size ratio and are given as $A = q^3 + 3q^2 + 3q$, $B = 3q^3 + 9q^2/2$, and $C = 3q^3$.

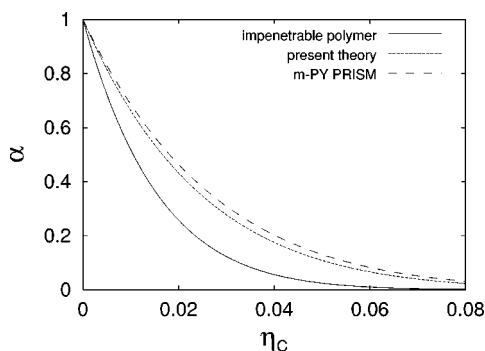


FIG. 2. Comparison of the free volume fraction α as a function of colloid packing fraction η_C and for size ratio $q=3$ for different models and approximations: Free volume theory for the AO model (solid line), present theory for the penetrable AO model (dotted line), m-PY PRISM approach (long-dashed line).

As pointed out in Sec. II, the PAO model reduces to the AO case for $\beta\epsilon_{CP} \rightarrow \infty$. In this limit, $\eta'_C = \eta_C$, and $\alpha_{PAO} = \alpha_{AO}$. As our DFT reduces to the corresponding functional for the AO model,^{20,21} we recover the same α_{AO} , which was strikingly shown to be equal to the expression for the free-volume fraction from the approach of Lekkerkerker *et al.*⁴ Hence our α_{PAO} generalizes the common free volume fraction to the case of penetrable colloid-polymer interactions.

Quantitatively, α_{PAO} significantly deviates from the free volume result, provided the size ratio q is large enough. We plot both quantities in Fig. 2 as a function of η_C for $q=3$, using the relation between size ratio and interaction strength in a theta solvent, $\beta\epsilon_{CP} = 3/q$. Except for the limiting value at $\eta_C=0$, significant deviations exist over the whole density range. These differences suggest significant deviations in the predicted phase behavior of both approaches—an issue that we will turn to in the next section.

In order to assess how well our α compares to the free volume fraction in real colloid-polymer mixtures, we consider the microscopic m-PY PRISM approach of Refs. 8–10. This theory was used to derive α from a description of polymers on the segment level [Eqs. (5) and (6) in Ref. 10]. We find that the free volume fractions from both approaches are similar, with α_{m-PY} being slightly larger. The deviations can be traced back to the fact that for large q and small η_C different expansions hold, namely $\alpha_{PAO} = 1 - 3\eta_C/q^2$ and $\alpha_{m-PY} = 1 - 2.42705\eta_C/q^2$.

B. Fluid demixing phase behavior

The conditions for phase equilibrium are equality of the chemical potentials of both species and of the total pressure in both phases. This is equivalent to performing a double tangent construction on the semigrand free energy where the polymer chemical potential is kept constant, see, e.g., Ref. 4 for further details.

We calculated binodals for the PAO model for size ratios $q=0.5, 1, 3, 10$ and display results in Fig. 3. For comparison we also show the binodals obtained from free volume theory for the AO model. Note that this predicts stable liquid-gas coexistence in the AO model for $q > 0.32$; for smaller values of q this transition becomes metastable with respect to the fluid-solid transition.^{4,5} Within our model both size ratio and colloid-polymer interaction strength are intimately coupled, hence by varying q , the interaction strength is $\beta\epsilon_{CP}$ varies. For the above sequence of q values, the colloid-polymer interaction strength in a theta solvent [given in Eq. (17)] takes on the values $\beta\epsilon_{CP} = 6, 3, 1, 0.3$, and the corresponding Boltzmann factor varies over a considerable range, namely $\exp(-\beta\epsilon_{CP}) = 0.00248, 0.0498, 0.368, 0.741$.

For $q=0.5$ [Fig. 3(a)] our binodals for both cases, theta solvent and good solvent, practically coincide (on the scale of the plot) with those for the AO model. This is due to the

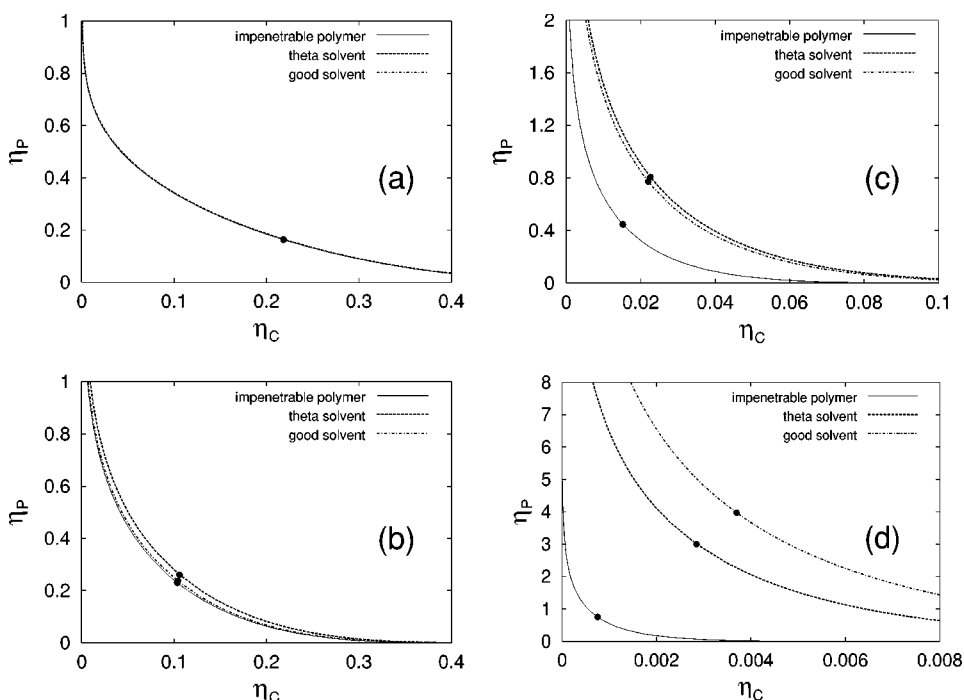


FIG. 3. Fluid-fluid demixing phase diagrams as a function of packing fractions η_C and η_P of colloids and polymers, respectively. Shown is the free volume result for the AO model with impenetrable polymer, along with the result of the present theory applied to the penetrable AO model for the cases of a theta solvent and a good solvent; the colloid-polymer interaction strength $\beta\epsilon_{CP}$ is prescribed by using Eq. (17) in the case of the theta solvent and by using Eq. (18) in the case of the good solvent. Dots represent the critical point. Different polymer-to-colloid size ratios q are shown: $q = 0.5$ (a), 1 (b), 3 (c), 10 (d).

fact that the Boltzmann factor for the cross interaction between colloids and polymers is tiny, hence penetrability is negligible. We conclude that both model and theory reduce to the correct limits. For $q=1$ [Fig. 3(b)] deviations begin to emerge. The binodal in the PAO cases is shifted upward to higher (polymer) fraction, leading to a stabilization of the mixed phase. Physically this is reasonable because the two different species repel each other weaker than in the AO case as the colloidal particles can now penetrate into the noncompact polymer coils. Stabilization of the mixed phase grows stronger upon increasing size ratio [see Figs. 3(c) and 3(d) for $q=3,10$]. For $q=10$ significant enhancement of the mixed phase is predicted. In the limit $q \rightarrow \infty$ for a theta solvent, we find that the critical point is at $\eta_C = 1/(3q^2) - 1/(2q^3)$, $\eta_P = q/3 - 1/2$ similarly as in Sear's recent blob-scaling extension of the free volume approximation of the AO model.⁷

V. CONCLUSIONS

Previous models of colloid-polymer mixtures employed interactions between polymer and colloid with a hard core, prohibiting overlap between colloids and polymers. This is a deficiency of these models, because in real systems, colloids may penetrate polymer coils, especially if the polymer radius of gyration is larger than the colloid size. In this work, we remedied this drawback by introducing a penetrable (finite for all distances) pair interaction between colloid and polymer. As a model, this was chosen to be a step-function and we have derived a geometry-based DFT and applied it to bulk fluid demixing. The free energy density is derived from the DFT by applying the functional to constant density profiles. The resulting analytical expression has a similar structure as the well-known free volume result.⁴ However, due to the penetrability, in the expression for the polymer free volume the bare colloid packing fraction η_C is replaced by a scaled packing fraction $\eta'_C = [1 - \exp(-\beta\epsilon_{CP})]\eta_C$ [see Eq. (21)], where $\beta\epsilon_{CP}$ is the strength of colloid-polymer repulsion. We determine the latter via virial coefficient arguments for the cases of a theta and a good solvent. When the size ratio $q > 1$, i.e., for long polymers $\beta\epsilon_{CP} \lesssim 1$, and hence η'_C differs markedly from η_C . As a consequence the free volume fraction is considerably larger than the classic result for impenetrable polymer⁴ and agrees reasonably well with the result from the microscopic m-PY PRISM approach.⁸⁻¹⁰ Our model is still effective in the sense that details on the segment level of the polymers are ignored *a priori*, and thus its phase boundaries become less reliable for large polymer-to-colloid size ratios where they shift deep into the semidilute polymer concentration range. Here, presumably our neglect of polymer-polymer interactions is not reliable anymore when applied to experimental systems. Nevertheless the

model's prediction that, for large polymers, particle penetration into the polymer coils becomes important compared to the classical AO picture should prove robust and agrees with more microscopic approaches^{8,11} where excluded volume is taken into account on the segment level. Our model also captures changes in miscibility resulting from excluded volume swelling of the polymer coils when varying the solvent quality, as has been seen experimentally,¹⁰ albeit for somewhat different parameters.

ACKNOWLEDGMENTS

Alan R. Denton, Joseph M. Brader, and Henk N. W. Lekkerkerker are gratefully acknowledged for useful discussions. M.F. was supported by the Deutsche Forschungsgemeinschaft under Grant No. Fu 309/3 and through the SFB 563.

- ¹S. Asakura and F. Oosawa, J. Chem. Phys. **22**, 1255 (1954).
- ²A. Vrij, Pure Appl. Chem. **48**, 471 (1976).
- ³A. P. Gast, C. K. Hall, and W. B. Russell, J. Colloid Interface Sci. **96**, 251 (1983).
- ⁴H. N. W. Lekkerkerker, W. C. K. Poon, P. N. Pusey, A. Stroobants, and P. B. Warren, Europhys. Lett. **20**, 559 (1992).
- ⁵M. Dijkstra, J. M. Brader, and R. Evans, J. Phys.: Condens. Matter **11**, 10079 (1999).
- ⁶P. G. Bolhuis, A. A. Louis, and J. P. Hansen (unpublished).
- ⁷R. Sear, Phys. Rev. Lett. **86**, 4696 (2001).
- ⁸M. Fuchs and K. S. Schweizer, Europhys. Lett. **51**, 621 (2000).
- ⁹M. Fuchs and K. S. Schweizer, Phys. Rev. E **64**, 021514 (2001).
- ¹⁰S. Ramakrishnan, M. Fuchs, K. S. Schweizer, and C. F. Zukoski, J. Chem. Phys. **116**, 2201 (2002).
- ¹¹M. Fuchs and K. S. Schweizer, J. Phys.: Condens. Matter **12**, R239 (2002).
- ¹²E. J. Meijer and D. Frenkel, Phys. Rev. Lett. **67**, 1110 (1991).
- ¹³E. J. Meijer and D. Frenkel, J. Chem. Phys. **100**, 6873 (1994).
- ¹⁴E. J. Meijer and D. Frenkel, Physica A **213**, 130 (1995).
- ¹⁵A. A. Louis, R. Finken, and J. Hansen, Europhys. Lett. **46**, 741 (1999).
- ¹⁶A. A. Louis, P. G. Bolhuis, J. P. Hansen, and E. J. Meijer, Phys. Rev. Lett. **85**, 2522 (2000).
- ¹⁷R. Evans, in *Fundamentals of Inhomogeneous Fluids*, edited by D. Henderson (Dekker, New York, 1992), p. 85.
- ¹⁸Y. Rosenfeld, Phys. Rev. Lett. **63**, 980 (1989).
- ¹⁹P. Tarazona, Phys. Rev. Lett. **84**, 694 (2000).
- ²⁰M. Schmidt, H. Löwen, J. M. Brader, and R. Evans, Phys. Rev. Lett. **85**, 1934 (2000).
- ²¹M. Schmidt, H. Löwen, J. M. Brader, and R. Evans, J. Phys.: Condens. Matter (issue in honor of J.-P. Hansen) (to be published).
- ²²M. Schmidt, A. R. Denton, and J. M. Brader, (unpublished).
- ²³J. M. Brader, R. Evans, M. Schmidt, and H. Löwen, J. Phys.: Condens. Matter **14**, L1 (2002).
- ²⁴M. Schmidt, J. Phys.: Condens. Matter **11**, 10163 (1999).
- ²⁵M. Schmidt, Phys. Rev. E **63**, 010101(R) (2001).
- ²⁶Y. Rosenfeld, M. Schmidt, H. Löwen, and P. Tarazona, J. Phys.: Condens. Matter **8**, L577 (1996).
- ²⁷Y. Rosenfeld, M. Schmidt, H. Löwen, and P. Tarazona, Phys. Rev. E **55**, 4245 (1997).
- ²⁸P. Tarazona and Y. Rosenfeld, Phys. Rev. E **55**, R4873 (1997).
- ²⁹E. Eisenriegler, A. Hanke, and S. Dietrich, Phys. Rev. E **54**, 1134 (1996).
- ³⁰A. Hanke, E. Eisenriegler, and S. Dietrich, Phys. Rev. E **59**, 6853 (1999).